17th World Conference on Earthquake Engineering, 17WCEE

Sendai, Japan - September 13th to 18th 2020

IMPACT OF ALTERNATIVE SOIL-STRUCTURE INTERACTION MODELS ON FRAGILITY OF BUILDINGS WITH PILE FOUNDATIONS

F. Cavalieri[(1)], A. A. Correia[(2)], R. Pinho[(3,4)], H. Crowley[(5)]

[(1)] *Researcher, European Centre for Training and Research in Earthquake Engineering (EUCENTRE), Via Adolfo Ferrata 1, 27100 Pavia, Italy, francesco.cavalieri@eucentre.it*
[(2)] *Assistant Researcher, National Laboratory for Civil Engineering (LNEC), Av. do Brasil 101, 1700-066 Lisboa, Portugal, aacorreia@lnec.pt*
[(3)] *Professor, University of Pavia, via Adolfo Ferrata 5, 27100 Pavia, Italy, rui.pinho@unipv.it*
[(4)] *Consultant, Mosayk Ltd., via Fratelli Cuzio 42, 27100 Pavia, Italy, rui.pinho@mosayk.it*
[(5)] *Seismic Risk Consultant, 27100 Pavia, Italy, hcrowley.consultant@gmail.com*

Abstract

Recent earthquake occurrence in the northern Netherlands has been attributed to gas production activity in the Groningen field. The largest earthquake to date has been the Huizinge event of August 2012 with a magnitude Mw 3.53. In response to this induced seismicity, the operators of the field have been developing a comprehensive seismic hazard and risk model for the region.

A key component of the risk assessment involves the definition of fragility functions for each building type that has been identified within the region. Structural drawings were used to develop a multi-degree-of-freedom (MDOF) numerical model of the structural system including the predominant non-structural elements. To reduce the computational effort in deriving fragility functions, a simplified single-degree-of-freedom (SDOF) equivalent system approach is used herein to analytically represent the structural system of each typology.

It is well known that dynamic Soil–Structure Interaction (SSI) may affect the fragility estimate, especially for soft soils and when soil nonlinearity is taken into account. This paper shows the impact of alternative SSI models on the assessment of seismic fragility functions for unreinforced masonry buildings with pile foundations. The substructure approach is initially adopted by implementing two different models, the first of which is one-dimensional and includes only a translational elastic spring and a dashpot, whose stiffness and viscous damping are retrieved from the real and imaginary parts of the dynamic impedance at the first natural frequency of the structure. The second and more refined model is a Lumped-Parameter Model (LPM), accounting for frequency dependence of the impedance through the introduction of fictitious (non-physical) masses in the interface node representing the foundation. Rocking-sway coupling is also considered. In order to explore the sensitivity of fragility functions to the linearity assumption, an additional approach, including soil nonlinearities, is employed. A nonlinear pile-head macro-element is introduced to model both the (inelastic) near-field and the (elastic) far-field response, condensing the entire soil-foundation system into a single nonlinear element at the base of the superstructure, which also accounts for energy dissipation through radiation damping. The comparison between the adopted approaches is evaluated in terms of their effects on the characterisation of collapse fragility functions.

Keywords: Induced seismicity; Lumped-Parameter Model; Macro-element; Soil nonlinearity; Multiple-stripe analysis.

1. Introduction

Regional risk assessment studies involve the definition of fragility functions (which describe the probability of exceeding a given damage or collapse state, conditional on the intensity of input ground motion), for each building typology that has been identified within the region of interest and included in the exposure model. If the mechanical properties of the soil on which such buildings are founded are such that soil-structure interaction (SSI) cannot be disregarded a-priori, then the derivation of fragility functions needs to take SSI into account.

In order to derive fragility functions through the undertaking of nonlinear dynamic analyses (e.g. Crowley et al., 2017 [1]), hundreds of records must be considered, rendering unfeasible the employment of finite element soil-block modelling strategies, due to their ensuing very significant computational burden. The latter is exacerbated further if there is a need to consider and model soil nonlinearity, in cases of very low resistance of the soil, such as that in the case-study region considered in this work (see Section 3). As such, the possible employment of an alternative more computationally efficient SSI modelling solution had to be identified, with three non soil-block SSI approaches being thus studied. The first two, namely a one-dimensional frequency-independent model and a two-dimensional Lumped-Parameter Model (LPM) accounting for frequency dependence of the coupled horizontal and rotational impedances, belong to the linear substructure approach, considering kinematic and inertial interaction effects by the principle of superposition. Instead, the third approach relies on the adoption of a nonlinear pile-head macro-element (Correia and Pecker, 2020) [2] and belongs to the class of hybrid methods, combining the features of sub-domain decomposition and finite element modelling, including soil nonlinearities.

2. Investigated index buildings

Three different index buildings modelled by Arup (2017a, 2019) [3][4] and featuring pile foundations have been considered herein, with the characteristics summarised in Table 1. These residential buildings are apartment blocks, all constructed with concrete floors and cavity URM walls (see Fig. 1).

Table 1 – Summary of the URM index buildings with pile foundations

Index Building Name	System type	Floor type	Wall type	# storeys	Mass (tonnes)
Drive-in	Apartment block	Concrete	Cavity	Garage + 2	764
Koeriersterweg (K-Flat)	Apartment block	Concrete	Cavity	3 + 2 attics	1493
Delfzijl (S-Flat)	Apartment block	Concrete	Cavity	4	2096

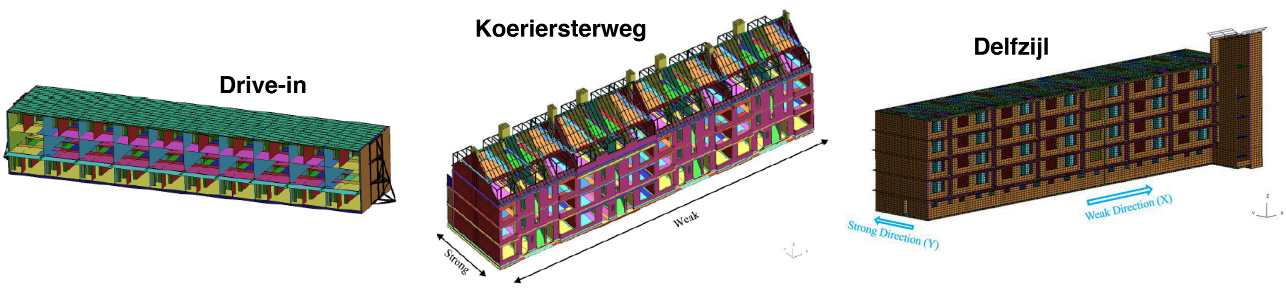

Fig. 1 – Screenshots of LS-DYNA models of URM index buildings with pile foundations

In all SSI models considered in this work, the superstructure is represented in a simplified way as a SDOF system, whose behaviour is described in SeismoStruct (Seismosoft, 2019) [5] with the use of the *multi_lin* model by Sivaselvan and Reinhorn (1999) [6]. The latter, characterised by a polygonal hysteresis loop, can simulate the deteriorating behaviour of strength and stiffness. In order to calibrate this hysteretic model, fixed-base MDOF models for each index building were produced in LS-DYNA (LSTC, 2013) [7] and were subjected to nonlinear dynamic analyses using 11 training records (see Arup, 2017b [8] for further details). The maximum attic displacement of a given MDOF model under each training record was converted to the equivalent SDOF displacement (see Crowley et al., 2019 [9]) and then compared with the displacement obtained under the same records for the fixed-base SDOF model in SeismoStruct. The logarithms of these displacements (*Sd*) were plotted against the logarithm of the average spectral acceleration (*AvgSa* - Bianchini et al., 2009 [10]) of each record, defined as the geometric mean of ten spectral accelerations from 0.01 to 1 seconds, and the linear regressions of each model compared. Afterwards, the SDOF model was iteratively adapted until a reasonable match was obtained (see Fig. 2).

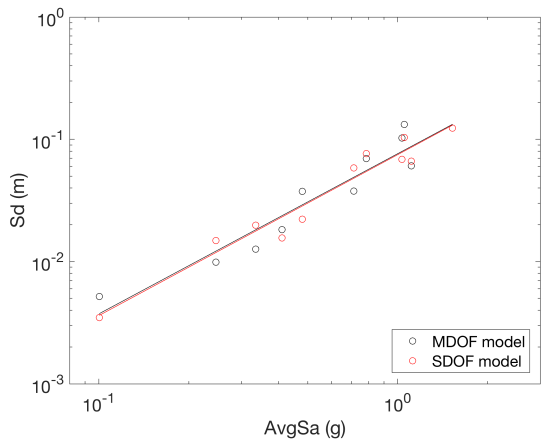

Fig. 2 – Comparison of displacements from MDOF (transformed to SDOF) LS-DYNA model and SDOF SeismoStruct model with calibrated *multi_lin* hysteretic model

3. Soil characterisation in Groningen

In order to account for SSI it is first required to define representative soil profiles that may be used for assessment of the input parameters of the different models used (one-dimensional frequency-independent, LPM, macro-element). The selection of representative soil profiles takes advantage of the detailed microzonation carried out in recent years for the Groningen region, resulting among others in maps of the site response Amplification Factor (AF) for several spectral ordinates (Rodriguez-Marek et al., 2017) [11]. A representative shear wave velocity (V_S) profile was evaluated as the mean of V_S profiles around the median AF (equal to 2.25) considering all sites with AFs in an interval of amplitude equal to 0.2 (see Fig. 3a) The AFs corresponding to the largest input motion level were considered. The V_S profile is not the only relevant parameter for SSI, therefore a real stratigraphy, with the corresponding soil parameters (strength, stiffness, etc.), needs to be identified. The simplest way to perform this operation is to identify a real stratigraphy (i.e. one of the about 140k sites considered for site response analyses) compatible with the computed mean V_S profile. This was done evaluating the deviation between the mean V_S profile and each one of the V_S profiles in the interval of median AF considered. Fig. 3b) shows the comparison between the mean V_S profile and the V_S profile with minimum deviation. The upper 30 m of the selected soil deposit is constituted by an alternation of fine sand and cohesive layers (i.e. clayey sand and sandy clay). In the shallow part, there is a 5 m thick layer of fine sand. The shallow water table level implies analysing the seismic pile response in undrained conditions.

In the framework of site response analysis, several soil parameters were associated to each site. Besides the V_S profile and soil stratigraphy, other geotechnical parameters used for site response analysis are included; in particular, a set of geomechanical parameters important to describe the dynamic soil behaviour, the modulus reduction and damping curves, are typically available (see Kruiver et al., 2017 [12] and Rodriguez-Marek et al., 2017 [11]). Unfortunately, for the fine sand surficial layer, strength parameters are not available;

consequently, they were defined based on existing literature, trying to constrain the selected values based on available information (i.e. V_S profile, coefficient of uniformity and D_{50}, diameter of the particles with 50% of passage in the grain size distribution). In particular, Fear and Robertson (1995) [13] proposed a framework for estimating the undrained steady state shear strength of sand (s_u) from *in situ* tests; the formulation combines the theory of critical state soil mechanics with shear wave velocity measurement. Fig. 3c) shows the undrained shear strength profile in the shallow part of the selected representative soil profile.

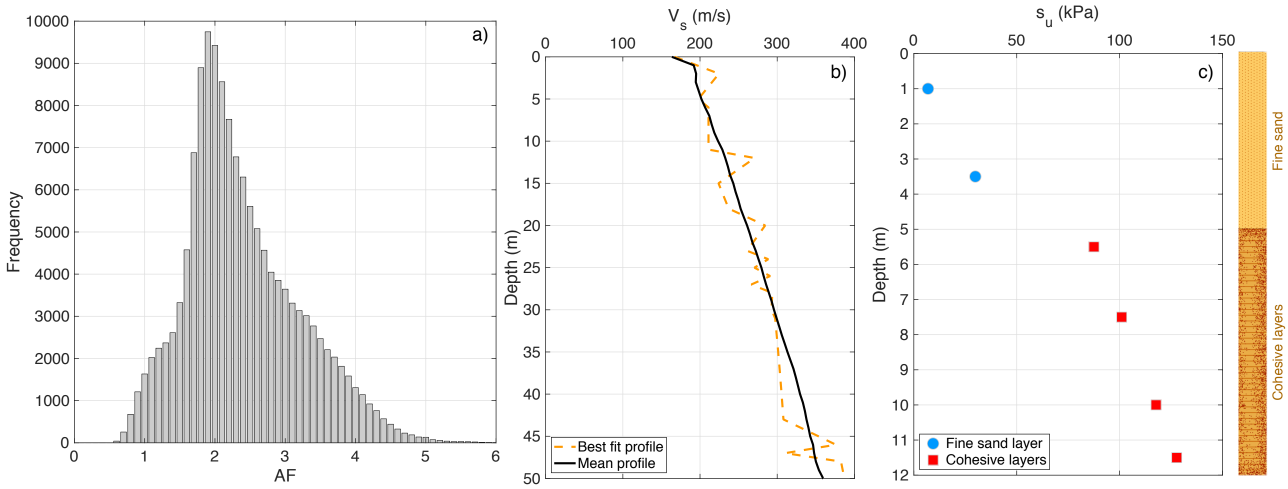

Fig. 3 – a) Histogram of AF at a period equal to 0.5 s and highest input motion level; b) Mean shear wave velocity profile around median AF *vs* best fit profile. Plots were derived using data described in Kruiver et al. (2017) [12] and Rodriguez-Marek et al. (2017) [11]; c) Undrained shear strength in the shallow part of the representative soil profile

4. Substructure approach

As mentioned already, in this work SSI was initially analysed by the substructure approach, which allows splitting kinematic and inertial interaction in different sub-steps and considering their combined effects using the principle of superposition (Mylonakis et al., 2006) [14]. In this study, kinematic interaction was deemed negligible in the response of the simplified models used for the definition of fragility curves. As a consequence, the free-field motion was used as input motion for the nonlinear dynamic analyses. Two different models following the substructure approach were implemented in SeismoStruct for derivation of fragility functions; they are described in Sections 4.2 and 4.3.

4.1 Definition of impedance functions

Impedance functions were evaluated using the software DYNA6.1 (GRC, 2015) [15], which for pile foundations allows the use of a layered medium. The depth interested by the presence of piles (i.e. 16 m) is subdivided into three layers, while the soil with thickness of 4 m below the pile tip is considered as a base layer. The shear wave velocity and the unit volume weight (γ) of each layer are equal to the average value within the stratum. Fig. 4a) represents the V_S profile of the layered medium considered. For each layer, the Poisson's ratio is taken equal to 0.45 and the material damping coefficient is assumed equal to 0.02. Based on the results of site response analysis, scaling factors (SF) for the V_S profile were defined to account for soil nonlinearity depending on the strain level. A relationship between peak ground acceleration (PGA) and V_S scaling factors was obtained considering at different PGA levels the mean strain level and shear modulus (G) degradation in the upper 20 m layers. Fig. 4b) shows the G/G_{max} scaling factors for the nine shear modulus degradation curves considered. Five PGA levels ranging from 0.05 g to 0.43 g were considered in the derivation of impedance functions. Further information can be found in Cavalieri et al. (2020a) [16].

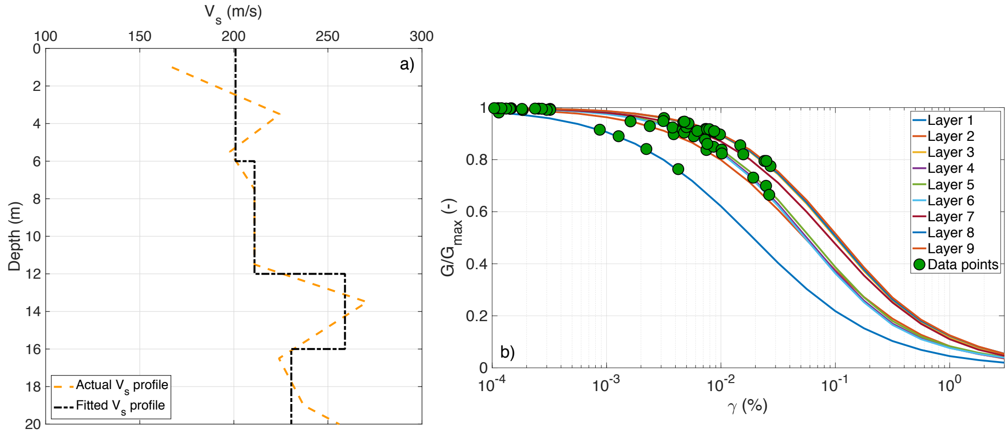

Fig. 4 – a) V_S profile of the upper 20 m of soil (dashed red line) and V_S profile considered for the layered medium used for computation of impedance functions of pile foundations; b) $G/G_{\max}$ scaling factors obtained from site response analysis for different levels of shear strain in the upper 20 m of soil layers, for the different shear modulus degradation curves considered

4.2 One-dimensional frequency-independent model

The simplest SSI model employed in the fragility functions' development in this work is a one-dimensional frequency-independent model, called SSI 1-D hereafter, having a lateral spring with stiffness k_x and a dashpot with viscous damping coefficient c_x. The values of the stiffness and viscous damping coefficient were obtained using the fundamental frequency of the fixed-base SDOF model together with the impedance functions derived for the Groningen field. The structural SDOF mass, stiffness and damping coefficient are indicated with m_s, k_s and c_s, respectively, in Fig. 5. The seismic excitation is input to the system as an acceleration time history, $a(t)$, applied to the fixed support at the base.

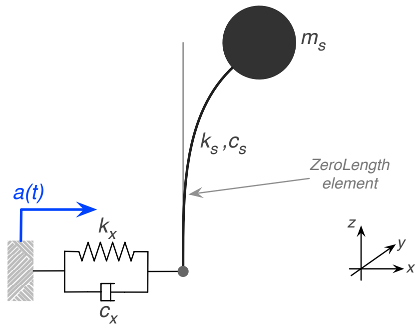

Fig. 5 – The adopted one-dimensional frequency-independent model

4.3 Lumped-Parameter Model (LPM)

A Lumped-Parameter Model (LPM) accounting for frequency dependence of the impedance functions was also implemented in SeismoStruct and used for the derivation of fragility functions. Even though techniques are available to describe frequency dependence of any type through a generalised LPM whose form is not known in advance (Lesgidis et al., 2015) [17], this work adopted the simplest LPM capable of describing approximately, over the frequency range of interest, the features of three components of impedance, namely the translational, rotational and roto-translational terms. The LPM model proposed by Dezi et al. (2009) [18] and Carbonari et al. (2011, 2012, 2018) [19][20][21] was adopted and implemented (see Fig. 6).

The crucial feature of this LPM is the introduction of a translational fictitious (non-physical) mass m_x in the interface node (representing the foundation), linked to the ground by a translational spring (of constant k_x) and by a dashpot (of constant c_x). This system is characterised by a frequency-dependent response to an input and thus allows for an approximate description of the frequency dependence of the impedance. Expressing the equation of motion of the system without the superstructure in the frequency domain, it can be easily seen that the dynamic impedance decreases parabolically ($k_x - m_x\,\omega^2$) with frequency, whereas the imaginary part increases linearly ($c_x\,\omega$) with frequency. In case the foundation mass is taken into account, it is added to the fictitious mass in the same node. In order to model the foundation rotation, the LPM includes a rotational mass m_{ry} in the interface node, linked to the ground by a rotational spring (of constant k_{ry}) and dashpot (of constant c_{ry}). Finally, rocking-sway coupling is achieved by adding a translational mass, spring and dashpot ($m_{x,ry}$, $k_{x,ry}$, $c_{x,ry}$), connected to the interface node by three rigid links of length h_m, h_k and h_c.

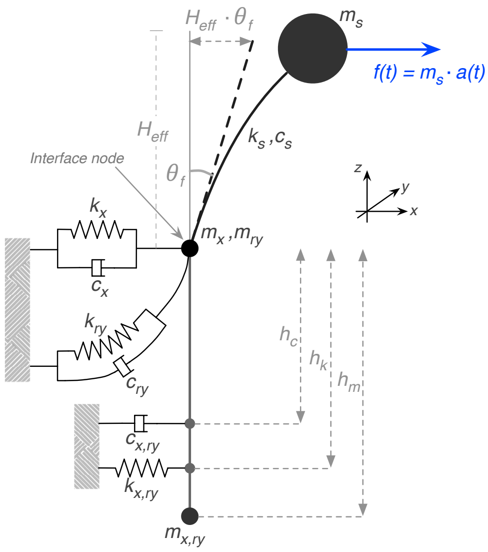

Fig. 6 – The adopted Lumped-Parameter Model for pile foundations

The soil portion of the LPM is characterised by three degrees of freedom, but only two of them are independent, due to the presence of rigid links. The model is comprised of nine equations with twelve unknowns, and hence the heights h_m, h_k and h_c must be assigned arbitrarily. The nine terms of the mass, stiffness and damping matrices are obtained by fitting the available three components of impedance (translational, rotational and roto-translational) with parabolic and linear functions for the real and imaginary parts, respectively. Given the three matrices, the parameters of the soil portion of the LPM are then retrieved by assigning the three heights and using equations that can be found in Cavalieri et al. (2020a) [16]. In order to capture the inertial interaction effects between the superstructure and the foundation, the superstructure mass is placed above the ground at the building centroid height, H_{eff}, and is connected to the interface node by a rigid link. In this way, the rigid displacement of the superstructure mass due to the foundation rotation θ_f, and equal to $H_{eff}{\cdot}\theta_f$, is taken into account within the nonlinear dynamic analyses, and then subtracted from the total displacement. The seismic acceleration, $a(t)$, is actually input to the system as an inertia force history, $f(t)$, applied to the superstructure mass: this approach properly considers the inertial components in the presence of the structure (structure and foundation masses and their interaction), resulting in a response in terms of relative displacements with respect to the ground motion.

5. Hybrid approach with nonlinear macro-element

5.1 Overview of the employed nonlinear macro-element

The pile-head macro-element developed by Correia and Pecker (2020) [2] may be regarded as a lumped model located at the base of the superstructure that intends to represent the behaviour of the entire soil-foundation system. The macro-element is based on the three fundamental features of the response of laterally loaded piles: initial elastic behaviour, gap opening/closure effects and failure conditions. These three characteristic behaviours are all made compatible by using an inelastic model that accounts for the evolution from initial nonlinear elastic behaviour to full plastic flow at failure. Such inelastic model is based on a bounding surface plasticity theory formulation that ensures a smooth transition from the initial elastic pile-head response up to nonlinear behaviour and collapse.

This pile-head macro-element model represents the lateral behaviour of single vertical piles, subjected to a horizontal load and a moment, from the initial stages of loading up until reaching failure. The effects of vertical loading are not directly considered in this model except for its influence on the plastic moment of the pile cross-section. Otherwise, it is considered that the upper zone of the soil profile, until the depth at which the plastic hinge will form, only contributes to the lateral load resistance. The vertical load is assumed to be transferred to the surrounding soil below that depth, where there is no influence of gap opening effects.

The adopted system for nonlinear dynamic analyses, as modelled in SeismoStruct, composed of a nonlinear structural SDOF and a pile macro-element, is shown in Fig. 7. As done for the LPM, in order to capture the inertial interaction between the superstructure and the foundation (with mass m_f), the superstructure mass is placed above the ground at the building centroid height, H_{eff}. Similarly, the seismic acceleration, $a(t)$, is actually input to the system as an inertia force history, $f(t)$, applied to the superstructure mass. All the springs and dashpots present in the macro-element, except the torsional ones, which do not play a role in the analyses of interest, are visualised in the 2D scheme of Fig. 7. Their constants correspond to the stiffness and damping in the vertical (k_V, c_V), horizontal (k_H, c_H), rotational (k_M, c_M) and roto-translational directions (k_{HM}, c_{HM}).

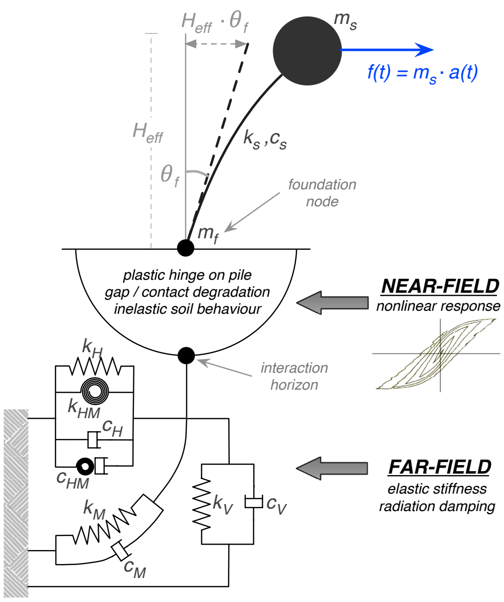

Fig. 7 – The adopted system with structural SDOF and pile macro-element

Since the structural model used for the computation of fragility curves is a SDOF model, the definition of the input parameters for a representative macro-element requires a calibration step. Such calibration was carried out in order to define the characteristics of the macro-element equivalent to the real foundation system. The calibration step, described in Section 5.3, was carried out considering a MDOF model for each building, in which each pile was represented by a macro-element, whose characteristics were defined as described in Section 5.2.

5.2 Assessment of input parameters for pile foundation macro-element

The approximate expressions for pile-head equivalent-linear impedances proposed by Gazetas (1991) [22] and adopted in EC8 – Part 5 (CEN, 2004) [23] , were assumed to be valid for representing the initial elastic dynamic stiffness of the macro-element. In relation to the shear wave velocity profile considered (see Fig. 4a), the formulation of pile-head impedance for constant soil stiffness with depth was considered. For the vertical stiffness component, in the case of a pile in a homogenous layer, the solution proposed by Mylonakys and Gazetas (1998) [24] was considered.

Gazetas (1991) [22] also presented the corresponding pile-head damping coefficients, which are computed for each frequency, *f*. These correspond only to the radiation damping component. Moreover, they are only valid for frequencies above the fundamental frequency of vibration of the soil deposit, since, if the bedrock is assumed to be rigid, no radiation damping exists below that frequency. Finally, the model specific parameters not discussed above were assigned values consistent with the calibration procedure done in the work by Correia (2011) [25]. Further information can be found in the report by Mosayk (2019) [26].

5.3 Properties of the equivalent macro-element

The employed pile macro-element models the soil under a single pile. However, given that the development of fragility functions is based on dynamic analyses of SDOF systems (Crowley et al., 2019) [9], the calibration of an "equivalent" pile macro-element was needed for all the investigated index buildings. To this end, the first step was to build in SeismoStruct two MDOF models. The first one is three-storey (see Fig. 8a) and was used for Drive-in and K-Flat, given the similarity of their geometric properties; only the total mass was changed accordingly. The second model is four-storey (see Fig. 8b) and was used for S-Flat. The two structural models only differ for the presence/absence of the fourth floor, given that the foundation plane was assumed to be the same for all the buildings, comprising a total of 67 piles distributed along the perimeter and five transversal axes along the *y*-direction, each of which modelled through a macro-element.

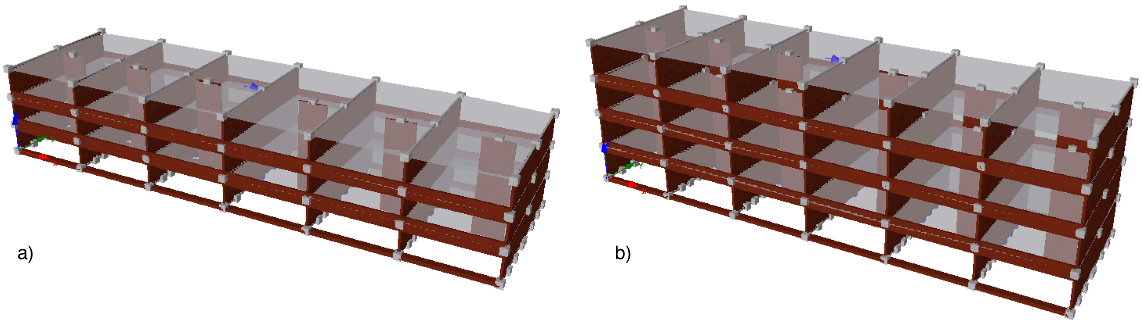

Fig. 8 – The MDOF models used for the investigated apartment index buildings: a) three-storey (for Drive-in and K-Flat); b) four-storey (for S-Flat)

The equivalent macro-element calibration requires the computation of the stiffness, capacity and damping along several directions. Most of the parameters were computed analytically starting from the foundation geometry and properties of the single macro-elements, while the remaining ones required the output from the models. The vertical stiffness, k_V, as well as the horizontal stiffness, k_H, were obtained by simply summing up the stiffness values of the single macro-elements, assuming a rigid behaviour of the foundation plane. The torsional stiffness, k_T, does not play a role in the fragility curve derivation since the models represent the response in a single vertical plane. For the rotational stiffness, k_M, an approach consisting in comparing the initial rotational stiffness of the MDOF model with the one of the simplified system composed of a nonlinear structural SDOF and an equivalent pile macro-element (see Fig. 7 above) was followed (see Cavalieri et al., 2020a [16]). Finally, the horizontal-rotational off-diagonal stiffness, k_{HM}, corresponds to the sum of reaction moments in the rotation-restrained upper nodes of macro-elements divided by the horizontal displacement of the base rigid plane.

Concerning the bearing capacity, the horizontal component, $H_{\max}$, was computed as the sum over the single macro-elements, while for the rotational component, $M_{\max}$, the procedure described below was employed. The pile-head failure surface is approximated by a rounded curve corresponding to a distorted superellipse, of equation (Correia et al., 2012) [27]:

$$\left|\frac{H_u}{H_{\max}} - \Gamma\frac{M_u}{M_{\max}}\right|^{n_H} + \left|\frac{M_u}{M_{\max}}\right|^{n_M} = 1 \qquad \text{with } M_u = \sum_{k=1}^{N_S} F_{u,k}\cdot h_k \tag{1}$$

where H_u is the ultimate base shear obtained from the pushover analysis, $F_{u,k}$ is the ultimate horizontal force at the k-th floor level, h_k, obtained considering a triangular distribution along the building height (N_S storeys), while n_H, n_M and Γ were set to 7.04, 2 and -0.667 (assumption of linear variation of undrained shear strength with depth), respectively. In Eq. (1), the only unknown is $M_{\max}$: the latter is derived from the ratio $M_u / M_{\max}$, which is obtained by interpolation in correspondence of the actual $H_u / H_{\max}$ value.

Concerning the radiation damping coefficients for the equivalent macro-element, they are defined in the vertical (c_V), horizontal (c_H) and rotational (c_M) directions. Similarly to the stiffness, a horizontal-rotational off-diagonal damping coefficient, c_{HM}, is also included in the set of damping parameters and requires a physical damper with coupled behaviour between the horizontal force and moment. Finally, the model specific parameters for the equivalent pile-head macro-element in SeismoStruct were set equal to those of the single pile-head macro-elements.

6. Fragility functions

6.1 Methodology

Hazard-compatible records for the development of fragility functions were selected through disaggregation of seismic hazard at four different return periods (T_r = 500, 2500, 10k and 100k years) at one of the highest hazard locations in the field. Four sets of 50 spectra, conditional on four different levels (corresponding to the four return periods) of *AvgSa*, were determined using the mean magnitude and distance from the disaggregation together with the 2017 ground motion and 5-75% significant duration prediction equations for the Groningen field (Bommer et al., 2017) [28]. The records were selected from a large database, including European and NGA-West records, to match both response spectra and 5-75% significant durations conditioned on four different levels of *AvgSa* (corresponding to the four return periods), using the ground motion selection procedure proposed by Baker and Lee (2018) [29], namely the Conditional Spectrum.

Using multiple-stripe analysis (MSA), for each of the four values of *AvgSa* (i.e. the stripes), the selected 50 records were used together with the SSI and SDOF models in SeismoStruct to calculate the maximum displacements. The logarithms of these displacements are plotted against the logarithm of *AvgSa* and then a censored linear regression is undertaken to obtain the parameters of the fragility functions (as shown in Fig. 9 and described further in Crowley et al., 2017, 2019 [1][9]).

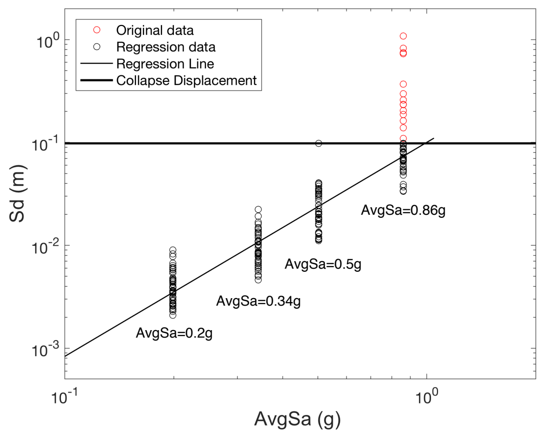

Fig. 9 – Example cloud data plot with linear censored regression of the dynamic displacement responses of the SSI + SDOF system (note: each vertical stripe corresponds, from left to right, to the results obtained using the T_r = 500, 2500, 10k and 100k year records, respectively)

6.2 Proposed fragility functions and comparison

Following the methodology presented in the previous Sections of the paper, fragility curves for the collapse limit state, for the three adopted SSI models and the three investigated index buildings were obtained, as shown in Fig. 10, where each subplot displays the curves related to: i) the simple one-dimensional elastic SSI case, ii) the LPM elastic SSI case, and iii) the nonlinear macro-element SSI case. The curve for the fixed-base case is also displayed for reference.

Unlike buildings with shallow foundations in Groningen, for which the influence of SSI was seen to be small to negligible (Cavalieri et al., 2020b) [30], these taller and stronger buildings are more affected by the rocking response of the foundation system, which is visible in the curves for the different SSI modelling approaches. A beneficial effect of SSI is quite visible for all the investigated index buildings. For the Drive-in building all three SSI-related fragility curves appear to be shifted to the right with respect to the fixed-base one (grey). In particular, while the two curves (blue and red) for the elastic models are not very distant from the fixed-base one, the (green) curve for the nonlinear macro-element is well separated on the right; this indicates that taking into account the nonlinear response of the foundation system, through the use of macro-elements, may have a non-negligible influence on the seismic vulnerability of buildings. The latter aspect is highlighted also in the case of the K-Flat building, for which only nonlinearity appears to bring a beneficial effect of SSI. For S-Flat, which is the heaviest and tallest building, as well as the less stiff one, the impact of nonlinearity on fragility curves is even more evident, being the macro-element-related curve very far on the right of the other ones. Similar to the cases of Drive-in and K-Flat, the two elastic curves are quite close to each other and to the fixed-base curve, with the LPM-related curve having the same median as the fixed-base one. As expected, the LPM-related curve is shifted to the right of the 1-D-related one, since the LPM model includes a rocking response, which is dominant for these buildings with pile foundations and, among the investigated buildings, especially for S-Flat.

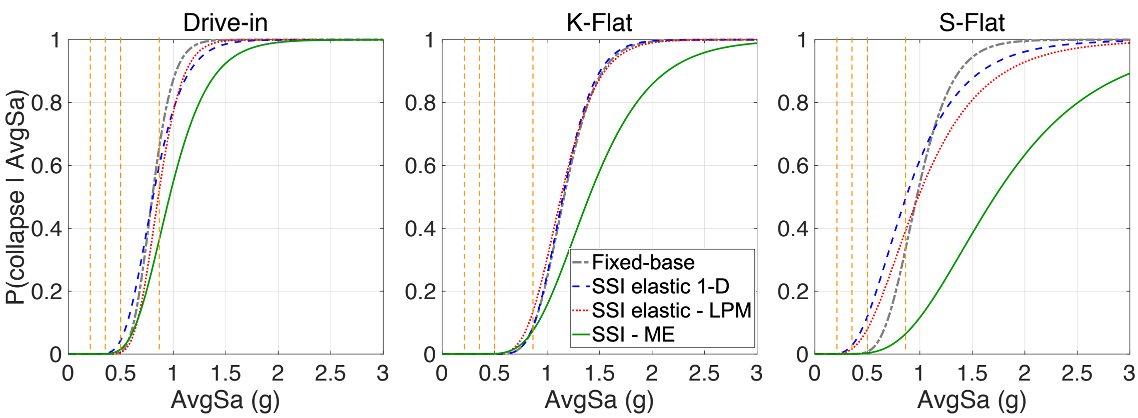

Fig. 10 – Proposed fragility curves for the investigated index buildings and the different SSI models. The orange dashed lines indicate the four considered levels of *AvgSa*; 0.2g (T_r = 500 years), 0.34g (T_r = 2500 years), 0.5g (T_r = 10k years) and 0.86g (T_r = 100k years)

In summary, based also on the results obtained for buildings with shallow foundations in Groningen (see Cavalieri et al., 2020b [30]), it is noted that for most buildings the consideration of inelastic SSI behaviour effectively leads to additional energy dissipation and, consequently, to smaller structural displacements. For this reason, the use of a nonlinear macro-element model is always recommended in the development of fragility functions.

7. Conclusions

In recent years, the Groningen region (northern Netherlands) has been affected by induced seismicity attributed to gas production activity. Within the comprehensive seismic hazard and risk model for the region developed by NAM, the definition of fragility functions for several URM index buildings is crucial. With reference to three of these representative buildings (considered here as SDOF systems) with pile foundations, this paper investigated the impact of adopting alternative models of SSI on the collapse fragility functions. Two of such SSI models, namely the one-dimensional frequency-independent and the LPM, are elastic, whereas the remaining one adopts a nonlinear macro-element to encompass all aspects of elastic (in the far-field) and inelastic (in the near-field) behaviour of the foundation system.

The paper showed that the influence of elastic SSI results to be small to negligible, whereas the inelastic SSI leads to fragility curves that are less unfavourable with respect to the fixed-base case, for all three buildings. This indicates that taking into account the inelastic behaviour of the soil-foundation system may lead to smaller structural displacements and hence to a lower vulnerability of the structures.

This work demonstrates that, in order to avoid the introduction of conservative bias in the results of risk assessment, it may be important not only to include SSI effects in the development of the fragility functions of the building stock, but also to adopt a nonlinear SSI model, especially for buildings founded on piles and thus affected by the rocking response of the foundation system. Such model, in the context of fragility functions derivation, where hundreds or thousands of nonlinear dynamic analyses need to be carried out, must necessarily be computationally effective like the macro-element, given that more refined approaches (involving e.g. the development of a 3D elasto-plastic soil-block model) have a computational cost that makes them unfeasible for such applications.

8. Acknowledgements

This work was undertaken within the framework of the research programme for hazard and risk of induced seismicity in Groningen sponsored by the Nederlandse Aardolie Maatschappij BV (NAM). The authors are particularly grateful to Pauline Kruiver, who kindly provided access to the soil mechanical characterisation data and site response analysis results for the Groningen region.

9. References

[1] Crowley H, Polidoro B, Pinho R, van Elk J (2017): Framework for developing fragility and consequence models for local personal risk. *Earthquake Spectra*, **33** (4), 1325–1345.

[2] Correia AA, Pecker A (2020): Nonlinear pile-head macro-element for the seismic analysis of structures on flexible piles. *Bulletin of Earthquake Engineering*, submitted for publication.

[3] Arup (2017a): EDB V5 Data Documentation. *Report n. 229746_052.0_REP2014*, NAM Platform (http://www.nam.nl/feiten-en-cijfers/onderzoeksrapporten.html), December 2017.

[4] Arup (2019): Typology modelling: Analysis results in support of fragility functions – 2018-2019 batch results, June 2019.

[5] Seismosoft (2019): *SeismoStruct 2020 – A computer program for static and dynamic nonlinear analysis of framed structures*, available at: http://www.seismosoft.com. Last accessed on 28 January 2020.

[6] Sivaselvan MV, Reinhorn AM (1999): Hysteretic models for cyclic behavior of deteriorating inelastic structures. Report MCEER-99-0018, MCEER. University of Buffalo.

[7] LSTC—Livermore Software Technology Corporation (2013): *LS-DYNA—a general-purpose finite element program capable of simulating complex problems*. Livermore.

[8] Arup (2017b): Typology modelling: analysis results in support of fragility functions—2017 batch results. *Report n. 229746_031.0_REP2005*, NAM Platform (http://www.nam.nl/feiten-en-cijfers/onderzoeksrapporten.html), November 2017.

[9] Crowley H, Pinho R, Cavalieri F (2019): Report on the v6 Fragility and Consequence Models for the Groningen Field. NAM Platform (http://www.nam.nl/feiten-en-cijfers/onderzoeksrapporten.html), March 2019.

[10] Bianchini M, Diotallevi P, Baker JW (2009): Prediction of inelastic structural response using an Average of Spectral Accelerations. *10th International Conference on Structural Safety and Reliability (ICOSSAR09)*, Osaka, Japan.

[11] Rodriguez-Marek A, Kruiver PP, Meijers P, Bommer JJ, Dost B, van Elk J, Doornhof D (2017): A Regional Site-Response Model for the Groningen Gas Field. *Bulletin of the Seismological Society of America*, **107** (5), 2067–2077.

[12] Kruiver PP, van Dedem E, Romijn R, de Lange G, Korff M, Stafleu J, Gunnink JL, Rodriguez-Marek A, Bommer JJ, van Elk J, Doornhof D (2017): An integrated shear-wave velocity model for the Groningen gas field, The Netherlands. *Bulletin of Earthquake Engineering*, **15** (9), 3555–3580.

[13] Fear CE, Robertson PK (1995): Estimating the undrained strength of sand: a theoretical framework. *Canadian Geotechnical Journal*, **32**, 859-870.

[14] Mylonakis G, Nikolaou S, Gazetas G (2006): Footings under seismic loading: Analysis and design issues with emphasis on bridge foundations. *Soil Dynamics and Earthquake Engineering*, **26** (9), 824-853.

[15] GRC - Geotechnical Research Centre of Western Ontario University (2015): *DYNA6.1 – A program for the computation of the response of rigid foundations to all types of dynamic loads*. Ontario, Canada, 2015.

[16] Cavalieri F, Correia AA, Crowley H, Pinho R (2020a): Seismic fragility analysis of URM buildings founded on piles: influence of dynamic soil-structure interaction models. *Bulletin of Earthquake Engineering*, submitted.

[17] Lesgidis N, Kwon OS, Sextos A (2015): A time-domain seismic SSI analysis method for inelastic bridge structures through the use of a frequency-dependent lumped parameter model. *Earthquake Engineering & Structural Dynamics*, **44** (13), 2137-2156.

[18] Dezi F, Carbonari S, Leoni G (2009): A model for the 3D kinematic interaction analysis of pile groups in layered soils. *Earthquake Engineering & Structural Dynamics*, **38** (11), 1281-1305.

[19] Carbonari S, Dezi F, Leoni G (2011): Linear soil–structure interaction of coupled wall–frame structures on pile foundations. *Soil Dynamics and Earthquake Engineering*, **31** (9), 1296-1309.

[20] Carbonari S, Dezi F, Leoni G (2012): Nonlinear seismic behaviour of wall-frame dual systems accounting for soil-structure interaction. *Earthquake Engineering & Structural Dynamics*, **41** (12), 1651-1672.

[21] Carbonari S, Morici M, Dezi F, Leoni G (2018): A lumped parameter model for time-domain inertial soil-structure interaction analysis of structures on pile foundations. *Earthquake Engineering & Structural Dynamics*, **47** (11), 2147-2171.

[22] Gazetas G (1991): *Foundation vibrations*, in *Foundations Engineering Handbook*, *2nd edition*, Fang H.Y. (Editor), New York, Van Nostrand Reinholds, pp. 553–593, chapter 15.

[23] CEN - Comité Européen de Normalisation (2004): *Eurocode 8: Design of structures for earthquake resistance - Part 5: Foundations, retaining structures and geotechnical aspects*. ENV 1998:5-2004.

[24] Mylonakis G, Gazetas G (1998): Settlement and additional internal forces of grouped piles in layered soil, *Geotechnique*, **48** (1), 55–72.

[25] Correia AA (2011): *A pile-head macro-element approach to seismic design of monoshaft-supported bridges*, Ph. D. thesis, European School for Advanced Studies in Reduction of Seismic Risk, (ROSE School), Pavia, Italy, 2011.

[26] Mosayk (2019): Calibration and verification of a nonlinear macro-element for SSI analysis in the Groningen region. *Report n. D14*, Mosayk, Pavia, Italy, April 2019.

[27] Correia AA, Pecker A, Kramer SL, Pinho R (2012): A pile-head macro-element approach to seismic design of extended pile-shaft-supported bridges. *Second International Conference on Performance-Based Design in Geotechnical Earthquake Engineering*, Taormina, Italy.

[28] Bommer JJ, Edwards B, Kruiver PP, Rodriguez-Marek A, Stafford PJ, Dost B, Ntinalexis M, Ruigrok E, Spetzler J (2017): V5 ground-motion model for the Groningen Field. NAM Platform, October 2017.

[29] Baker JW, Lee C (2018): An improved algorithm for selecting ground motions to match a conditional spectrum. *Journal of Earthquake Engineering*, **22** (4), 708-723, 2018.

[30] Cavalieri F, Correia AA, Crowley H, Pinho R (2020b): Dynamic soil-structure interaction models for fragility characterisation of buildings with shallow foundations. *Soil Dynamics and Earthquake Engineering*, in press.

